Aerothermodynamic Analysis of Aerocapture and Ballistic Entry Flows in Neptune's Atmosphere

João Alexandre Abreu Coelho

Supervisors

Prof. Mário Lino da Silva (ISTécnico, IPFN)
Prof. Domenic D'Ambrosio (PoliTo)

January 2021

Outline

Outline

TÉCNICO LISBOA

1. Mission Context

Neptune's Mission

- Neptune is a strong candidate for a joint class-M NASA/ESA mission (2030-2040) to our Solar System's Ice Giants (Uranus and Neptune)
- Neptune's atmosphere:
  - H_2 and He (~ 80%/20%)
  - CH_4 (~ 1.5%)
- Mission's Goal: reach final elliptic orbit which includes regular flybys on Triton (Neptune's moon)
  - Using atmospheric drag to slow the spacecraft

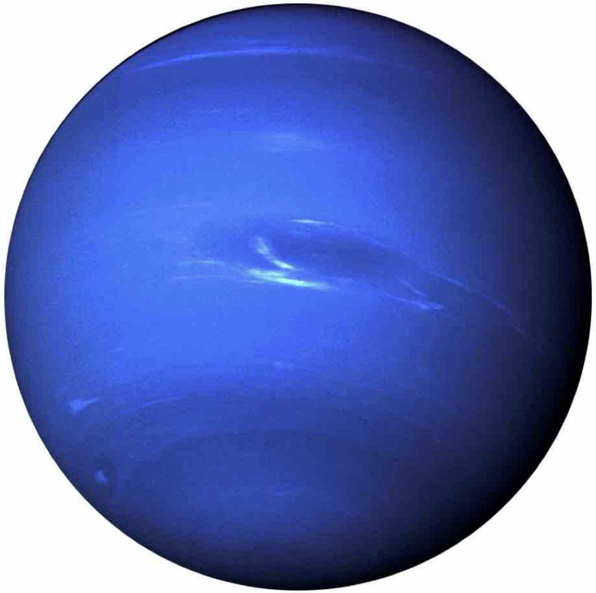

Credits: NASA

Aerocapture

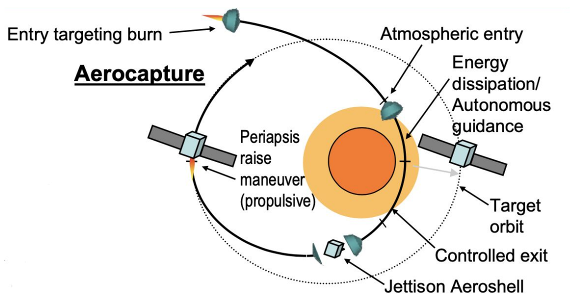

Aerocapture. [1]

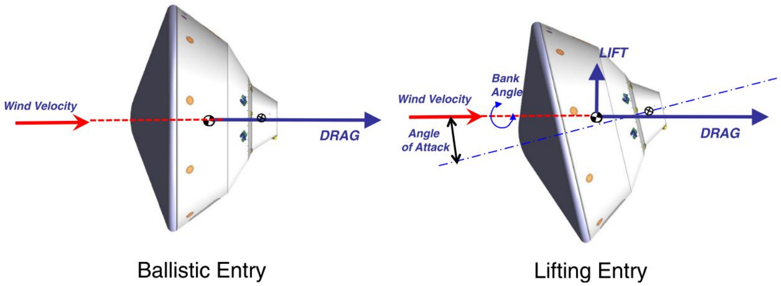

Ballistic vs Lifting entry [2]

Lifting entry ⇨ angle of attack

For controlled angle of attack, the most common systems are:

- Ballast mass
- Reaction Control Systems (RCS)
- Using **trim tab** (may increase mission's useful mass by 140%)

2. Objectives

Objectives

- Aerothermodynamic analysis for two trajectory points (TP)
  - (Ballistic) Entry TP and Aerocapture TP
  - Study capsule design and atmospheric compositions
  - Focus on convective and radiative wall heat fluxes

- Aerodynamic analysis for Aerocapture TP
  - Analyze aerodynamic coefficients
  - Check sweep angle influence

3. Aerothermodynamic Effects

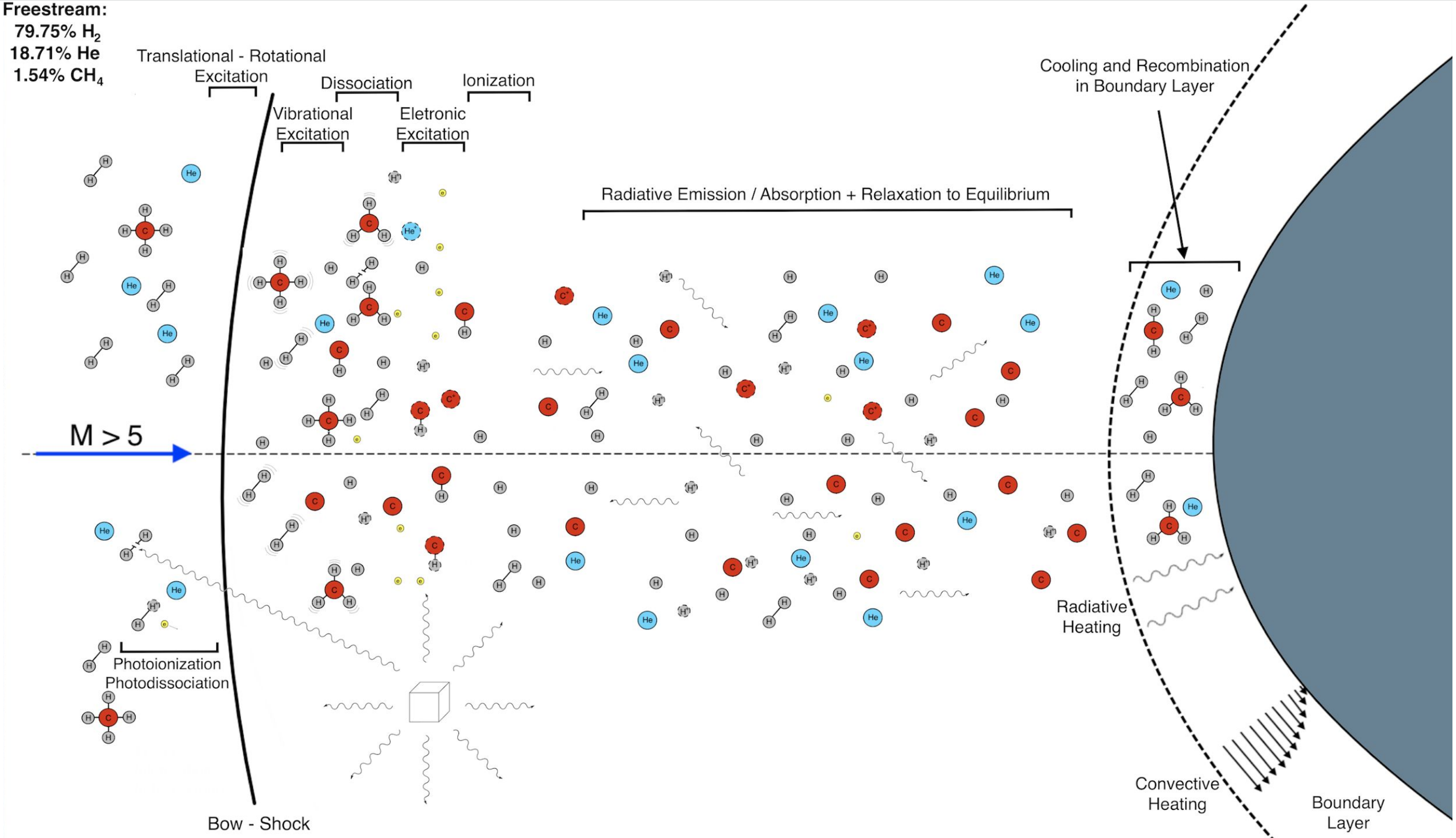

High-temperature effects in hypersonic flow (H_2 - He - CH_4 mixtures). Adapted from [3]

4. Capsule Design

Capsule Design

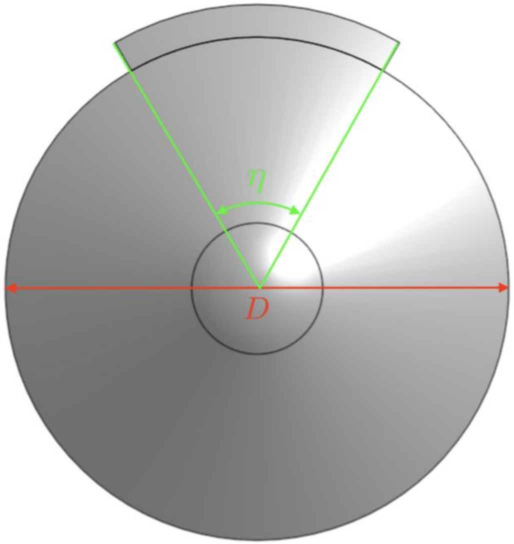

Capsule front view.

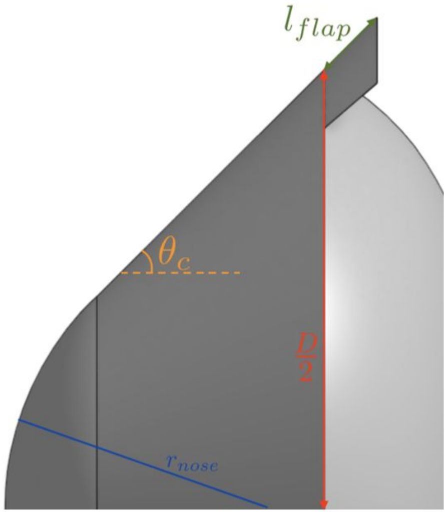

Capsule side view.

- θ_c cone angle
- D diameter
- r_{nose} nose radius
- η sweep angle
- l_{flap} trim tab's length

Capsule Design

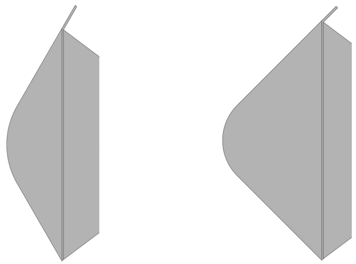

60° and 45° Capsules.

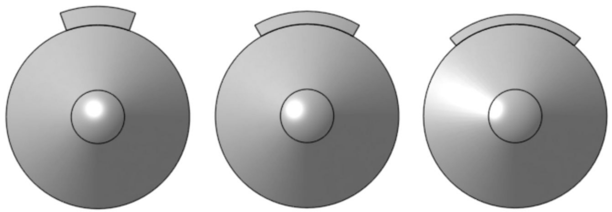

Flap's sweep angle (η).

θ_c	60°					45°				
$D\,[m]$	1.50					1.50				
$r_{nose}\,[m]$	$0.333 \cdot D = 0.500$					$0.205 \cdot D = 0.308$				
A_{flap}/A_{main}	5%					5%				
η	40°	50°	60°	70°	80°	40°	50°	60°	70°	80°
$l_{flap}\,[cm]$	17.68	14.39	12.14	10.50	9.24	21.66	17.63	14.86	12.85	11.32

Capsule dimensions.

5. Governing Equations

Navier Stokes Equations

- Mass conservation $$\frac{\partial(\rho c_s)}{\partial t} + \boldsymbol{\nabla} \cdot (\rho c_s \boldsymbol{V}) = \boldsymbol{\nabla} \cdot \boldsymbol{J_s} + \dot{w}_s$$
- Momentum conservation $$\frac{\partial(\rho \boldsymbol{V})}{\partial t} + \boldsymbol{\nabla} \cdot (\rho \boldsymbol{V} \otimes \boldsymbol{V}) = \boldsymbol{\nabla} \cdot [\boldsymbol{\tau}] - \boldsymbol{\nabla} p$$
- Energy conservation $$\frac{\partial(\rho e)}{\partial t} + \boldsymbol{\nabla} \cdot (\rho \boldsymbol{V} e) = \boldsymbol{\nabla} \cdot (\boldsymbol{V} \cdot [\boldsymbol{\tau}]) - \boldsymbol{\nabla} \cdot (p \boldsymbol{V}) - \boldsymbol{\nabla} \cdot \boldsymbol{q}$$

Navier Stokes Equations

- Mass conservation $$\frac{\partial(\rho c_s)}{\partial t} + \boldsymbol{\nabla} \cdot (\rho c_s \boldsymbol{V}) = \boldsymbol{\nabla} \cdot \boldsymbol{J_s} + \dot{w}_s$$
- Momentum conservation $$\frac{\partial(\rho \boldsymbol{V})}{\partial t} + \boldsymbol{\nabla} \cdot (\rho \boldsymbol{V} \otimes \boldsymbol{V}) = \boldsymbol{\nabla} \cdot [\boldsymbol{\tau}] - \boldsymbol{\nabla} p$$
- Energy conservation $$\frac{\partial(\rho e)}{\partial t} + \boldsymbol{\nabla} \cdot (\rho \boldsymbol{V} e) = \boldsymbol{\nabla} \cdot (\boldsymbol{V} \cdot [\boldsymbol{\tau}]) - \boldsymbol{\nabla} \cdot (p \boldsymbol{V}) - \boldsymbol{\nabla} \cdot \boldsymbol{q}$$

For each thermal non-equilibrium mode, adds:

$$\frac{\partial(\rho e_k)}{\partial t} + \boldsymbol{\nabla} \cdot (\rho \boldsymbol{V} h_k) = \boldsymbol{\nabla} \cdot \left(-\kappa_k \boldsymbol{\nabla} T_k + \sum_s \boldsymbol{J}_s h_{s,k} \right) + \dot{\Omega}_k$$

Non-Equilibrium Models

Thermal Non-Equilibrium

2T model with $T_{v,H2}$

Chemical Non-Equilibrium

Two chemical compositions studied:

Composition A freestream

- 79.8% H_2
- 18.7% He
- 1.5% CH_4

Composition B freestream

- 81.0% H_2
- 19.0% He
- 0.0% CH_4

	H_2	H_2^+	H	H^+	He	He^+	CH_4	CH_3	CH_2	CH	CH^+	C_2	C_2^+	C	C^+	e^+
A	•	•	•	•	•	•	•	•	•	•	•	•	•	•	•	•
B	•	•	•	•	•	•										•

Chemical species for each composition

Transport Model

- Gupta-Yos Model (1st and 2nd Order)
  - Mixing rule for all transport properties function of Collisional Cross Sections (CCS)
    - Viscosity
    - Thermal conduction
    - Diffusion

$$\left.\begin{matrix} \mu \\ k_k \\ D_s \end{matrix}\right\} = f\left(\Delta_{s,l}^{(1)}, \Delta_{s,l}^{(2)}\right)$$

$\Delta_{s,l}^{(1)}, \Delta_{s,l}^{(2)}$ function of CCS different for each interaction (s,l)

Heat Flux

$$\frac{\partial(\rho e)}{\partial t} + \boldsymbol{\nabla}\cdot(\rho \boldsymbol{V} e) = \boldsymbol{\nabla}\cdot(\boldsymbol{V}\cdot[\boldsymbol{\tau}]) - \boldsymbol{\nabla}\cdot(p\boldsymbol{V}) - \boldsymbol{\nabla}\cdot\boldsymbol{q}$$

$$\boldsymbol{q} = \boldsymbol{q}_D + \boldsymbol{q}_C + \boldsymbol{q}_R$$

$$= \sum_s \boldsymbol{J}_s h_s - \sum_k \kappa_k \boldsymbol{\nabla} T_k + \boldsymbol{q}_R$$

- Radiative heat flux neglected in the flowfield computations
- Flowfield and Radiation decoupled
- Radiative heat flux only computed at the wall

Radiative Heat Flux

$$q_R = \int_0^\infty \int_\Omega q_\nu \, d\Omega \, d\nu$$

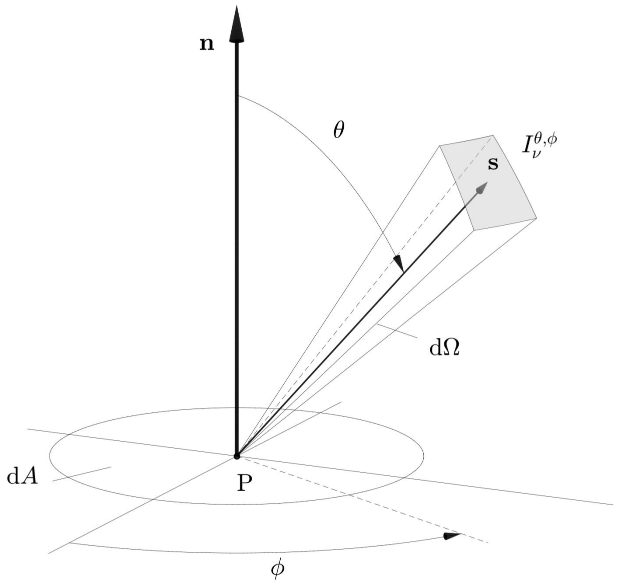

Retrieved from [3]

Spectral radiative heat flux

$$q_\nu = \int_{4\pi} I_\nu^{\theta,\phi} \boldsymbol{s} \cdot \boldsymbol{n} d\Omega$$

Beer-Lambert Law (Radiative Transfer Equation)

$$\frac{dI_\nu^{\theta,\phi}}{ds} = j_v - \kappa_\nu I_\nu^{\theta,\phi}$$

TÉCNICO LISBOA

6. Computational Framework

SPARK CFD Code

SPARK Code

Software Package for Aerodynamics Radiation and Kinetics

Software **P**ackage for **A**erodynamics **R**adiation and **K**inetics
Maintained **IPFN**

- Cell-centered finite volume formulation
- Euler and **Navier-Stokes** formulations
- Time discretization
  - **Implicit** and Explicit second-order
- Convective fluxes discretization
  - Second-order TVD **Harten-Yee** (with minmod flux limiter)
- Non-Equilibrium models (**chemical** and/or **thermal**)
- Multi-species chemically reacting flows
- Flowfield and radiation **uncoupled**

Computational Approach

- Axisymmetric flow
- 0º angle of attack (2D code limitations)
- Domain with flap ~ without flap
    - Assumption: flow is supersonic in the outlet:
        - Expansion do not need modeling, since its influence does not reach upstream

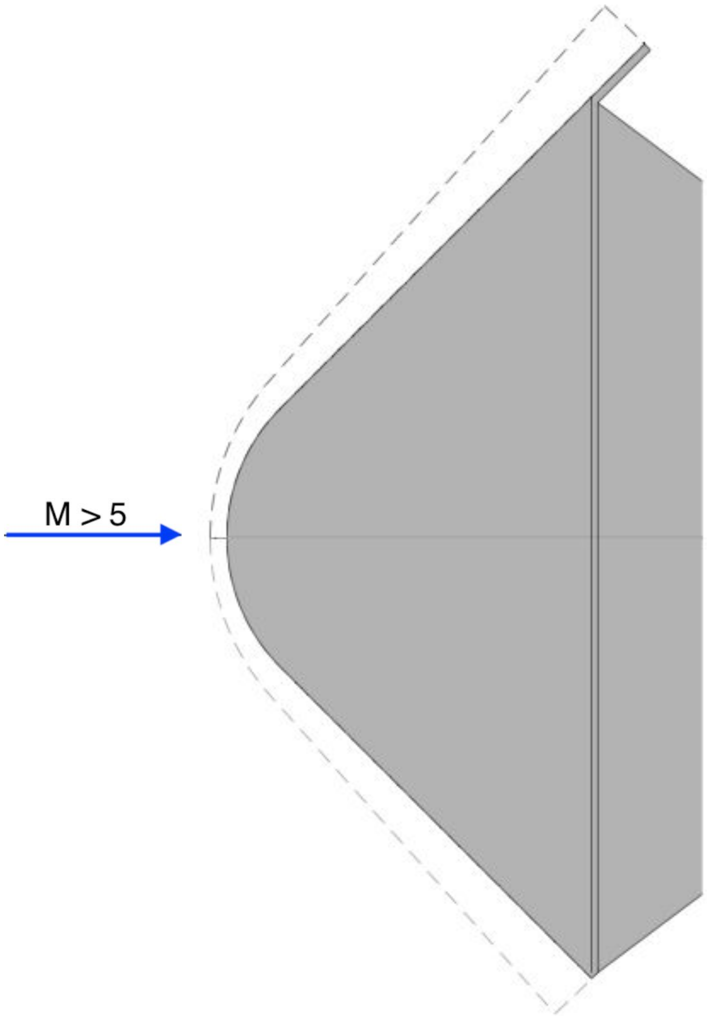

Mesh Boundaries

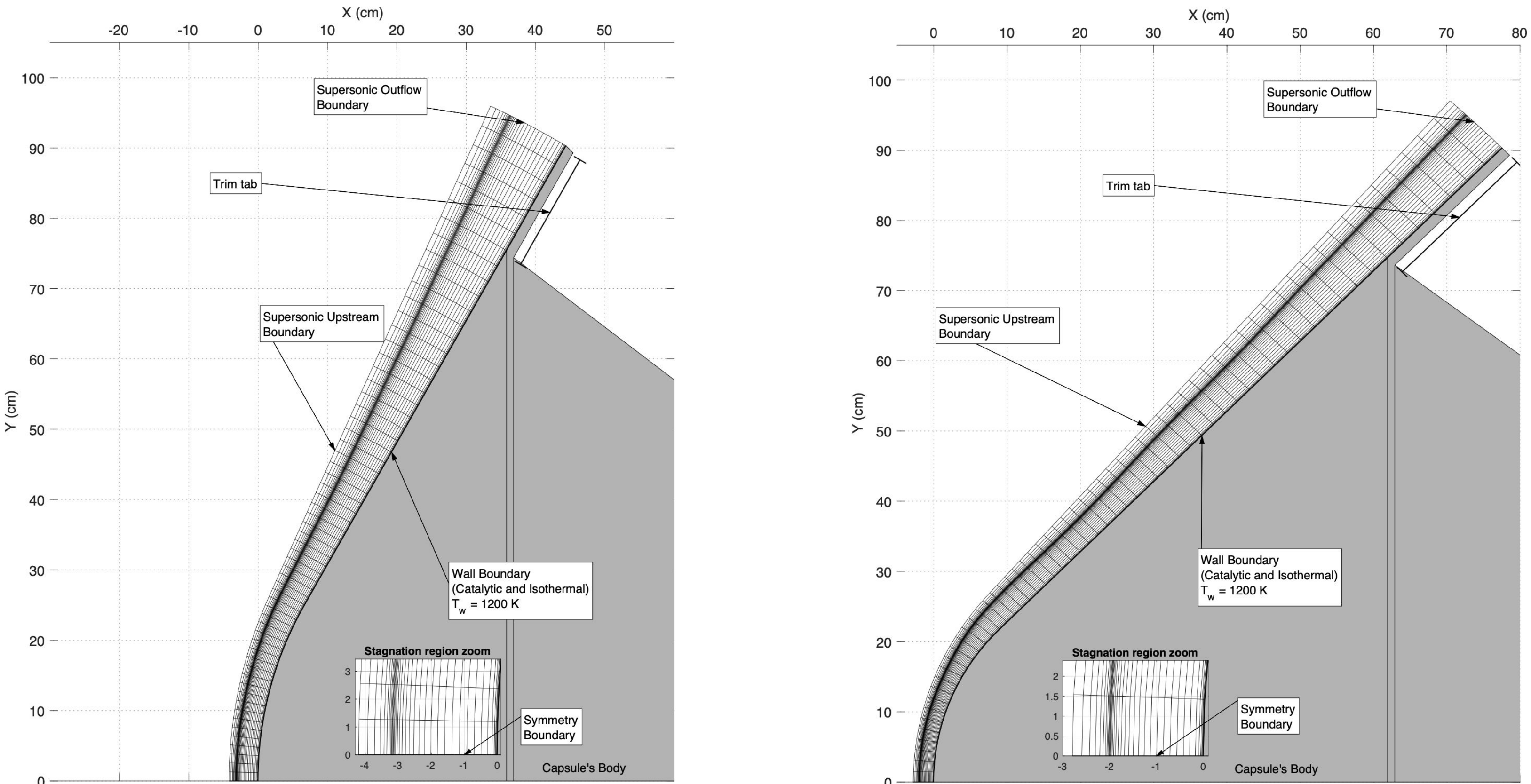

θ_c=60°

θ_c=45°

Mesh Study

- Mesh convergence study
    - 90 x 60 mesh
    - **70 x 60 mesh**
    - 50 x 60 mesh *

*for Radiative Study (computationally more expensive)

- Mesh refinement
    - Shock and Boundary Layer
    - Performed externally (MATLAB)

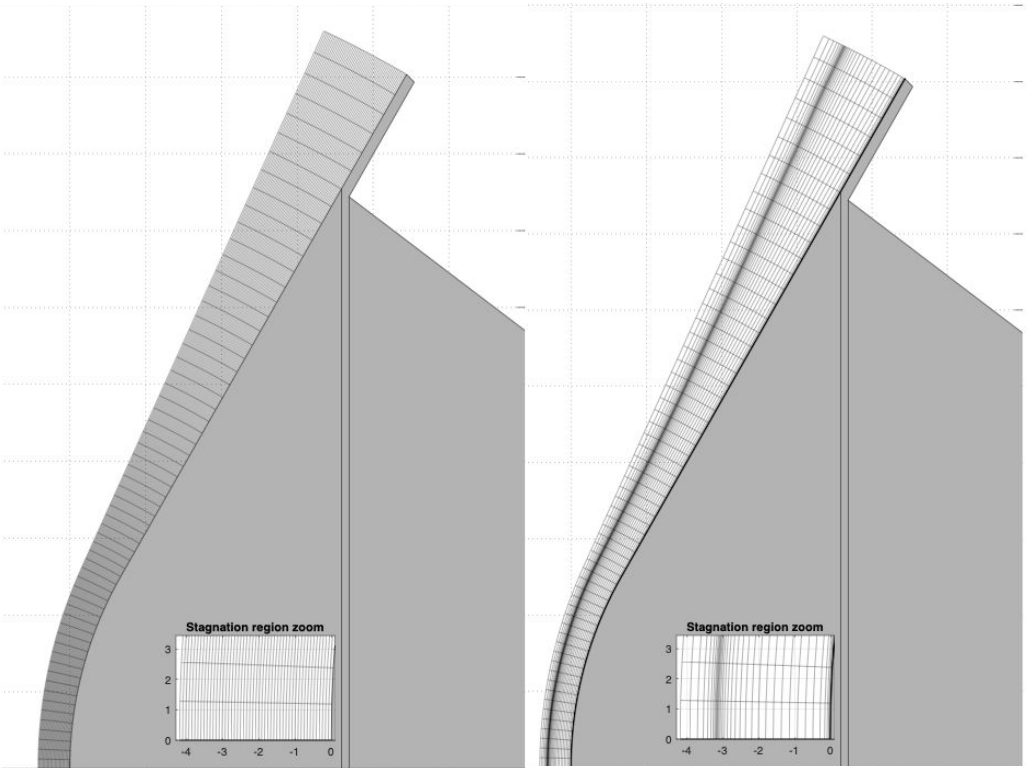

Mesh refinement example (θ_c=60°)

SPARK Line-by-Line Radiative Solver

SPARK Line by Line (LbL) Structure

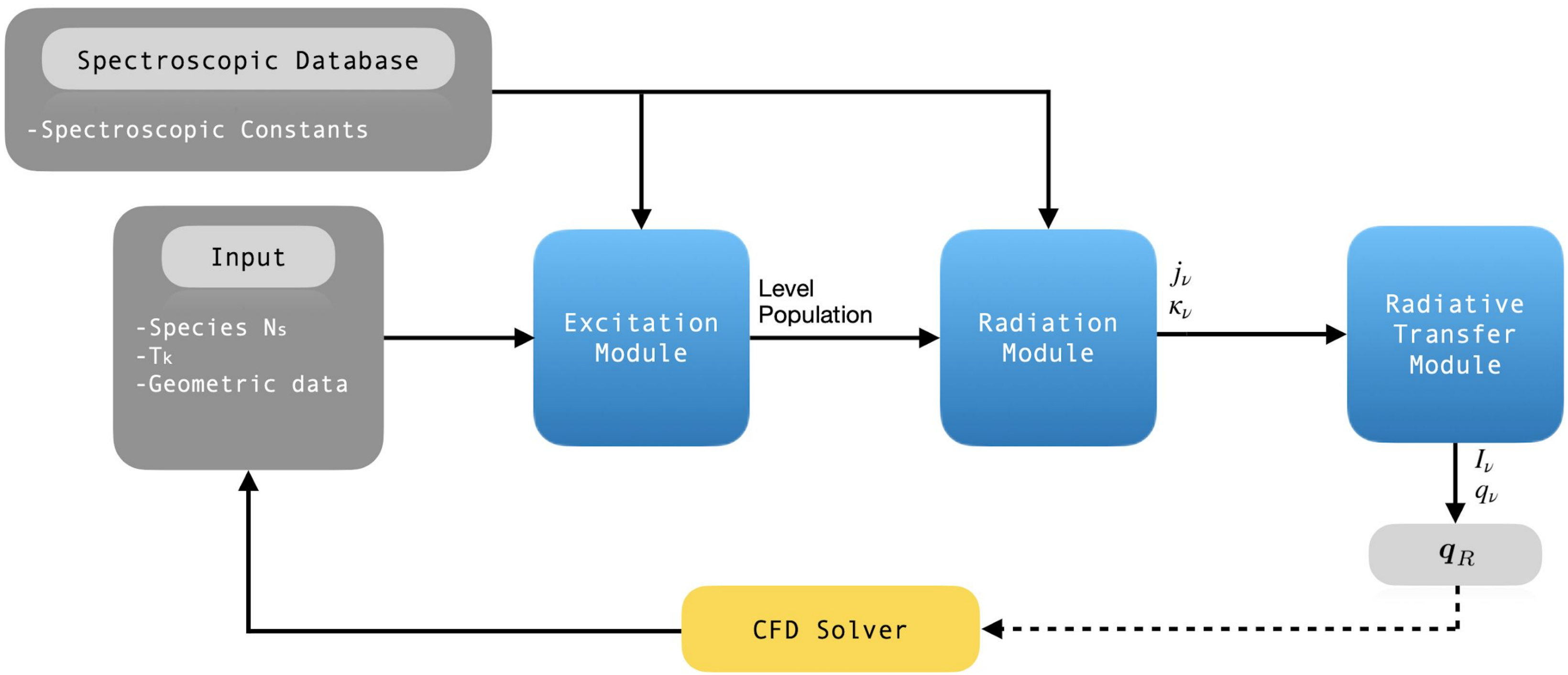

Tangent slab approach

- Spatial integration over one coordinate
- Overpredicts the radiative heating (5-20% in this work)
- Faster

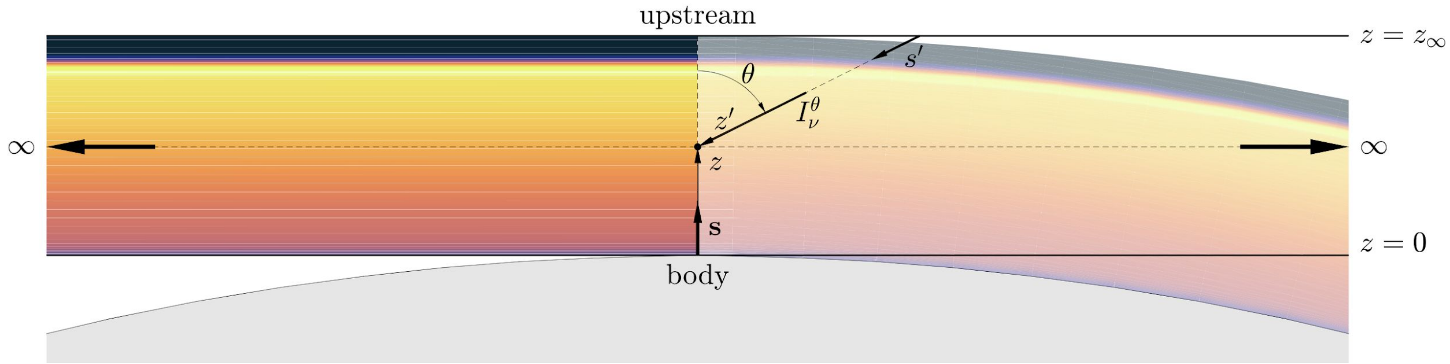

Tangent slab representation. [3]

Ray tracing model

- Solved along particular directions through different rays
  - Requires ray discretization
    - Ray distribution (Fibonacci lattice)

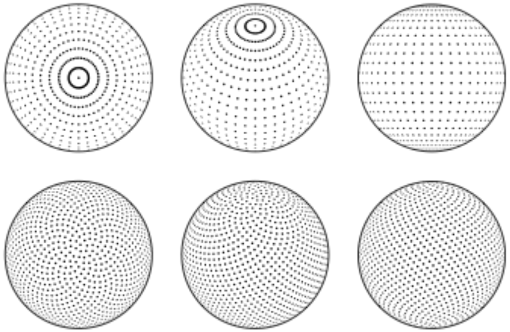

Latitude-longitude vs Fibonacci lattice. [8]

    - Convergence study
      - 50 rays present errors below 2.5% locally (compared with 1500 rays) and globally (compared with 150 rays)

7. Results

TÉCNICO LISBOA

Test case 1

Test case 1

Study CH_4 and **capsule design** influence in both in the **flowfield** results and **radiative** results.

- Focus on the wall convective and radiative heat fluxes

Two trajectory points (TP):

- (Ballistic) **Entry TP**
  - ESA CDF Study [5]
- **Aerocapture TP**
  - Hollis et al. [4]

	Entry TP		Aerocapture TP
Cone angle θ_c	$60°$	$45°$	$60°$ /$45°$
V [km/s]	18.05	18.27	29
p [Pa]	698	892	145
ρ [kg/m^3] (x10^{-3})	2.996	4.229	0.378
T [K]	74.5	66.5	120.3
h (from 1 bar) [km]	82.3	77.3	130

Freestream properties for both TP

Cone angle θ_c	Trajectory Point	Chemical Composition
60°	Entry TP	A (with CH_4) B (without CH_4)
45°	Entry TP	A (with CH_4) B (without CH_4)
60°	Aerocapture TP	A (with CH_4) B (without CH_4)
45°	Aerocapture TP	A (with CH_4) B (without CH_4)

Test Matrix for Test case 1

Sonic line transition

- Aerocapture TP for 60º: does not present supersonic outlet (with/without CH_4)

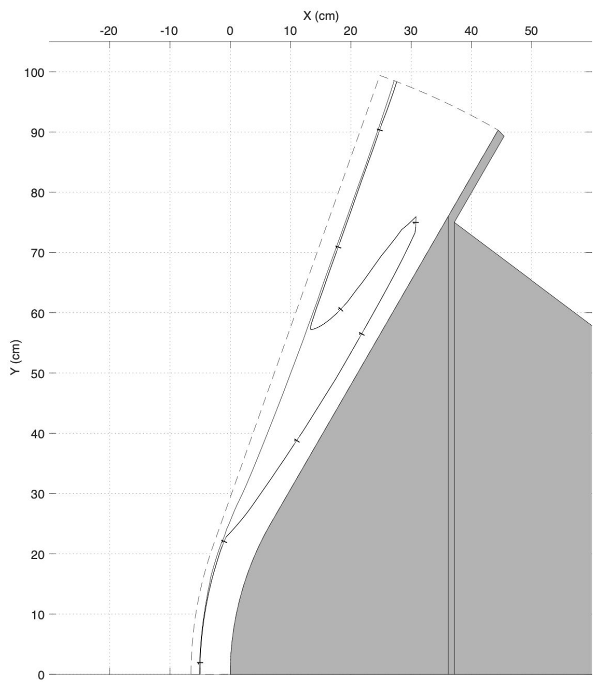

Sonic Line for Aerocapture TP θ_c=60º

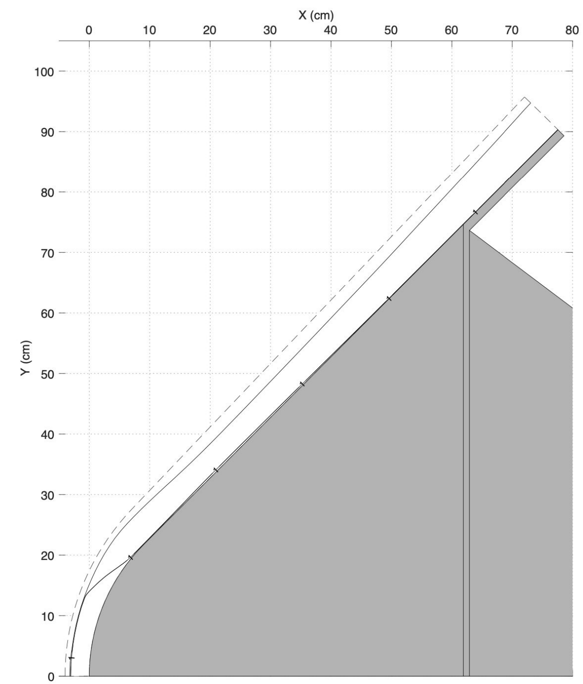

Sonic Line for Aerocapture TP θ_c=45º

Sonic line transition

- $\theta_c > \theta_s$
  - $\theta_s \rightarrow \theta$ when the sonic line attachment starts to move away from the spherical part of the capsule
    - $\theta_s = f(\gamma, M_\infty)$
    - γ post-shock varies with temperature

- Transition already happening for Entry TP
  - Not critical

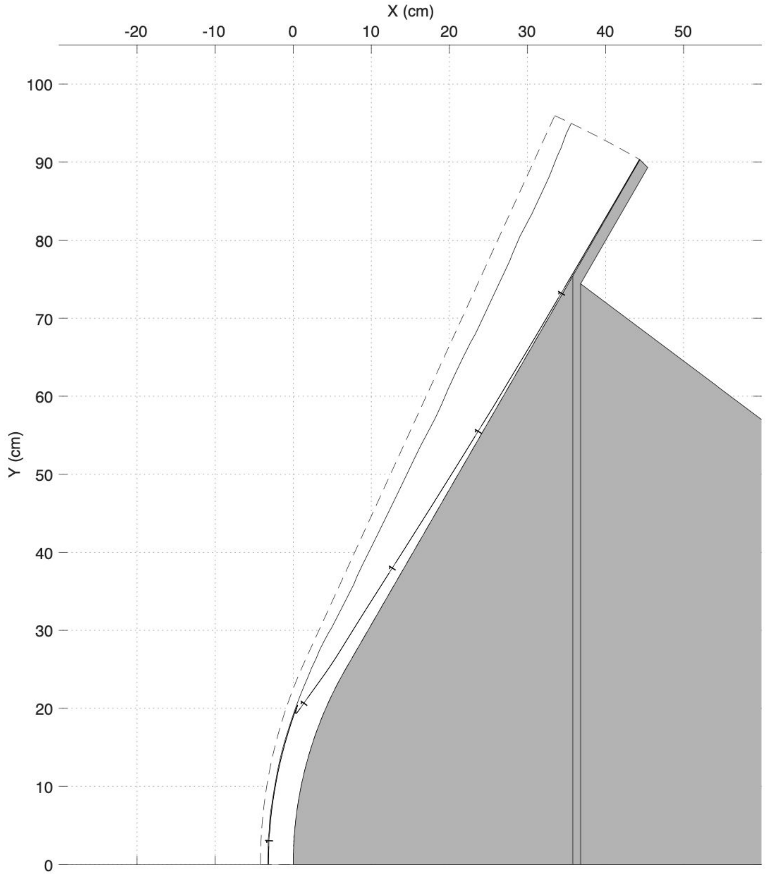

Sonic Line for Entry TP θ_c=60º

Sonic line transition

- Vary θ_c from 45° to 61° (keeping r_{nose} constant)
- Bubble created at θ_c=46°
- Expansion would be required starting from θ_c=52°, as the sonic line reaches the shoulder
- After joining the shock, the sonic line would attach in the expansion region as the flow accelerates
- Instabilities particularly when an angle of attack is considered

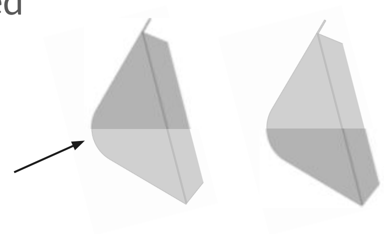

- Incorrect assumptions made *a priori*

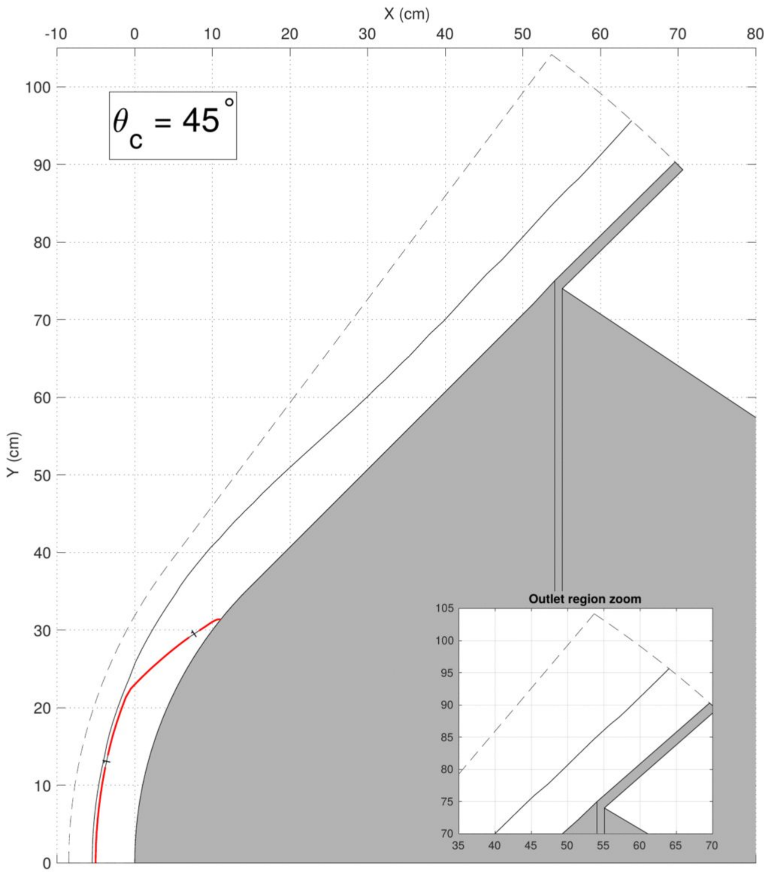

Sonic Line (red) for Aerocapture TP
from θ_c=45° to θ_c=61°
r_{nose} = 0.5m

Entry TP - Stagnation line

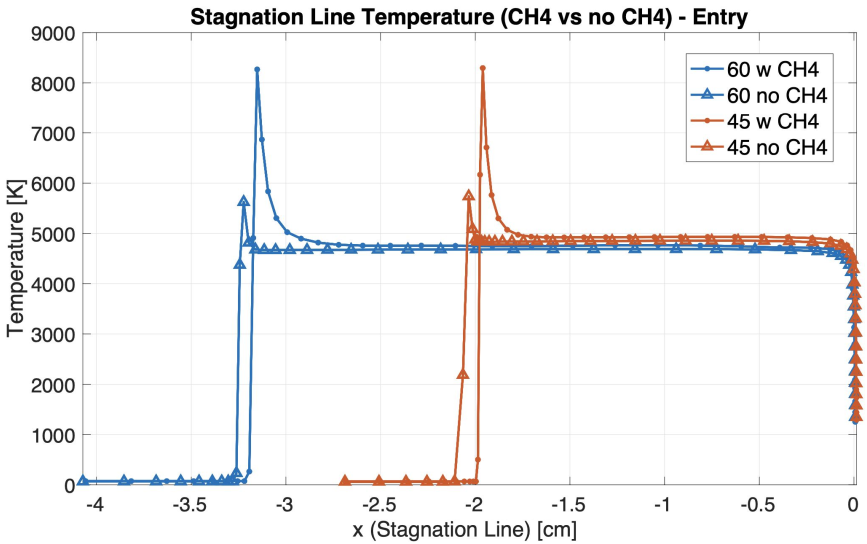

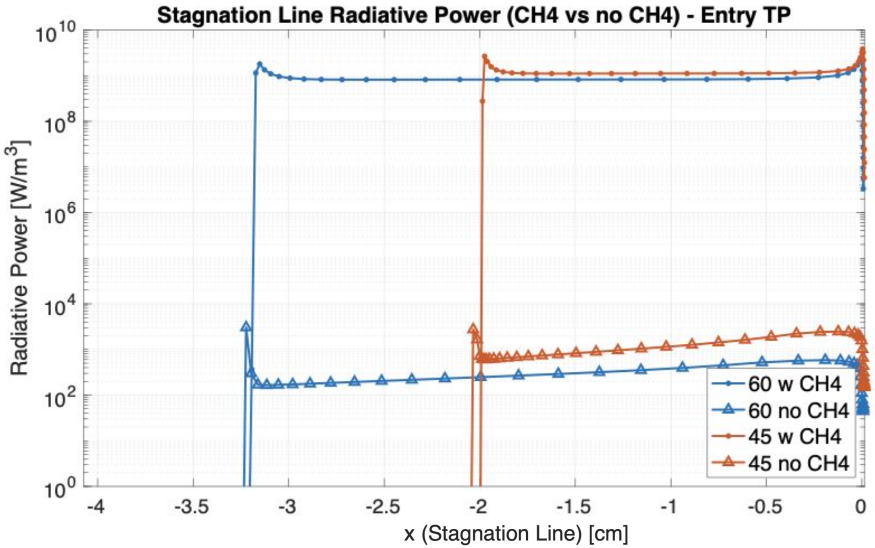

- Peak temperature ~ 8,000 K
- Equilibrium region temperature ~ 5,000 K

- Significant discrepancy in total radiative power between chemical compositions

Entry TP - Stagnation line

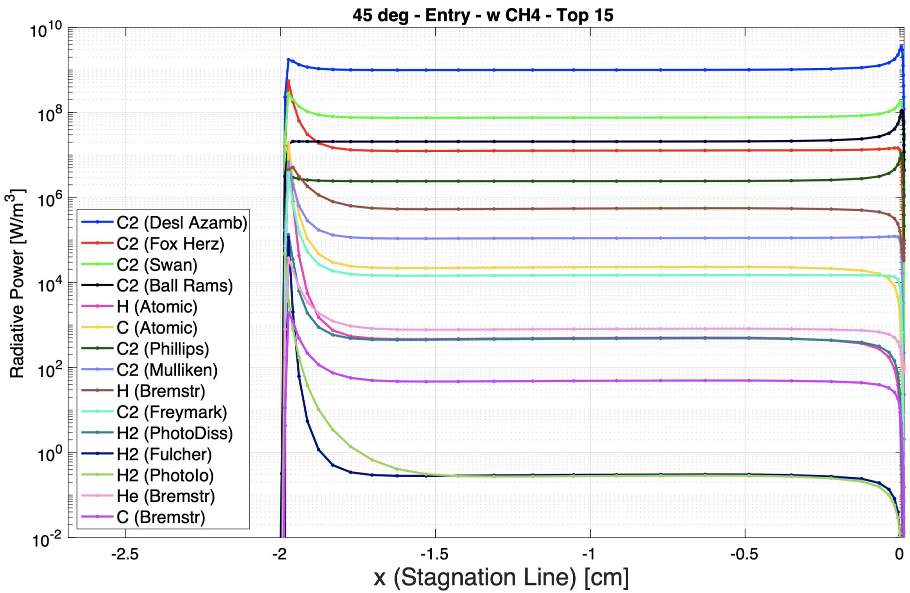

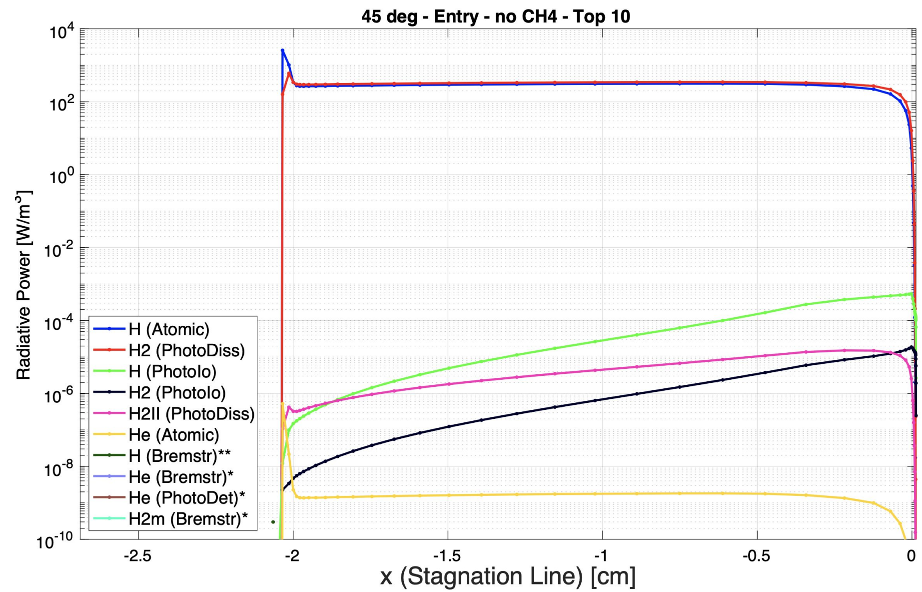

- C_2 transitions are dominant for chemical composition A
- H for chemical composition B (lower order of magnitude)

Aerocapture TP - Stagnation line

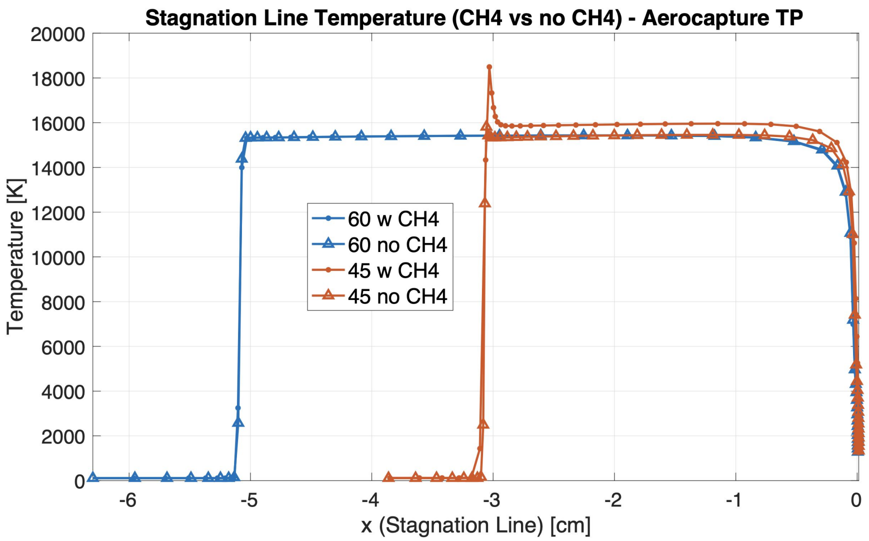

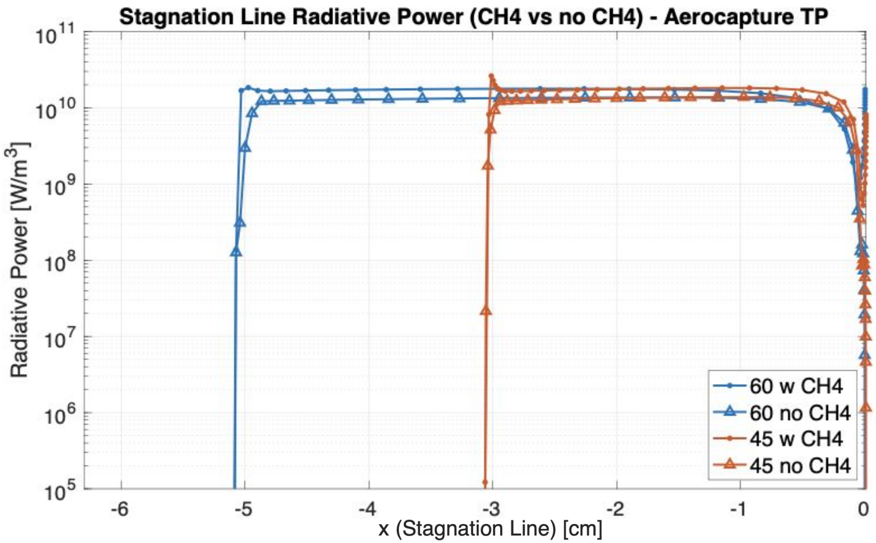

- Peak temperature ~ 18,500 K
- Equilibrium region temperature ~ 16,000 K

- Almost no difference in total radiative power between chemical compositions

Aerocapture TP - Stagnation line

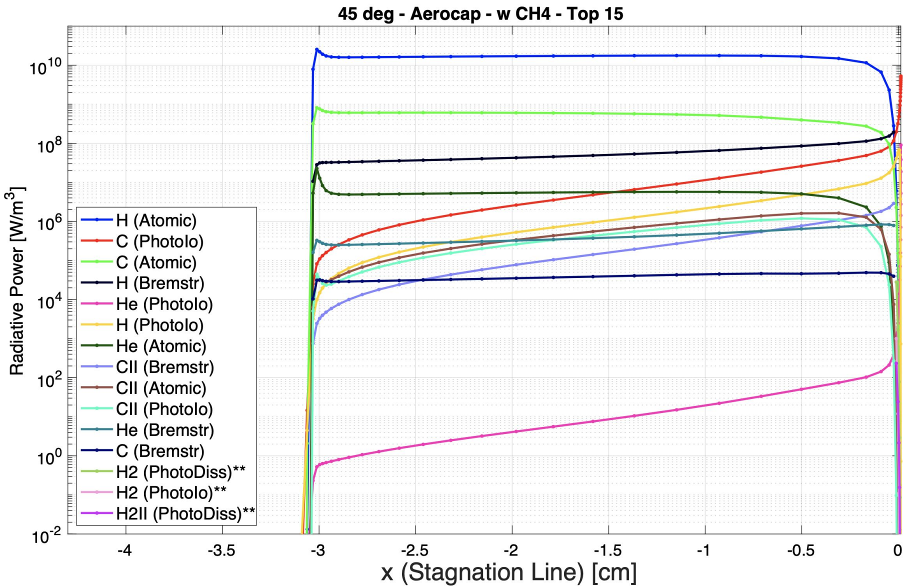

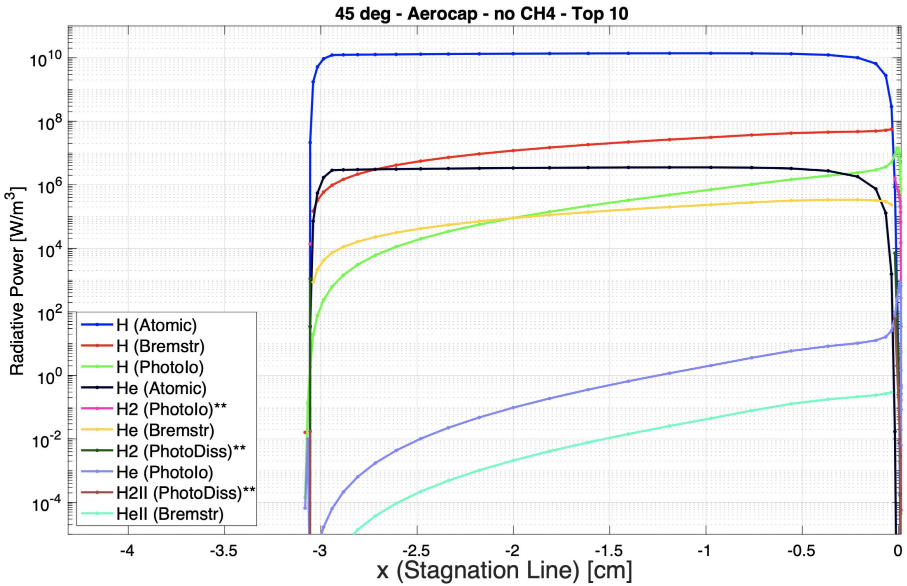

- Atomic H transitions is the dominant radiative system

Wall heat fluxes - Entry TP

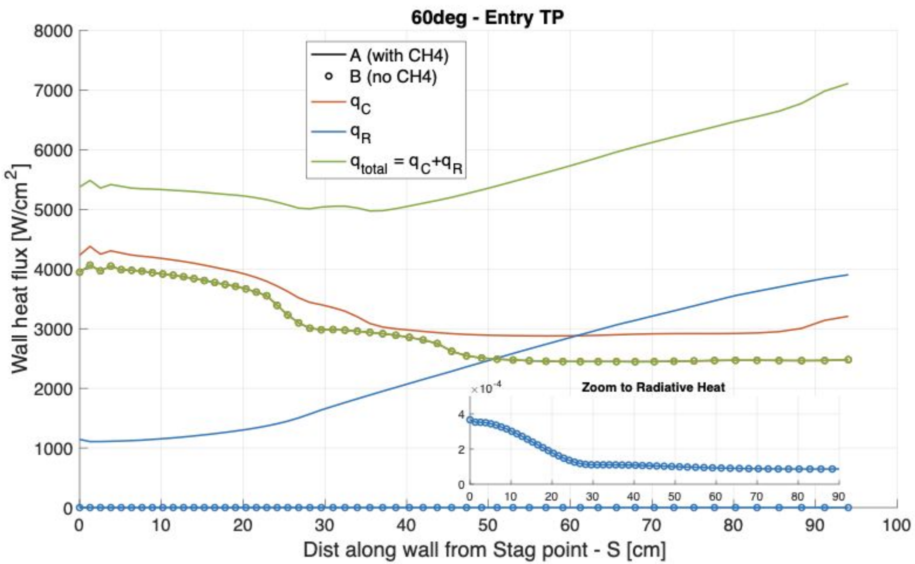

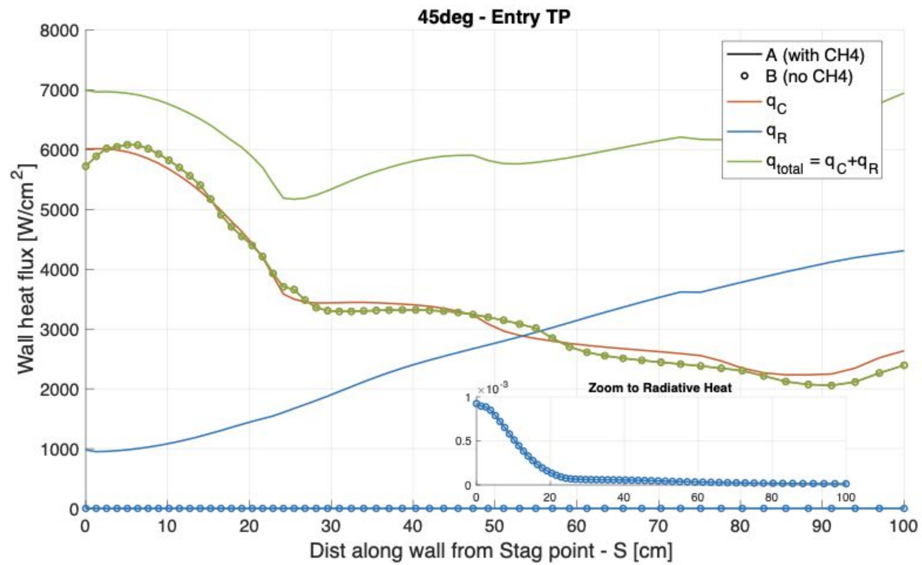

- Convective heat fluxes with similar results between chemical compositions
- Significant difference in radiative heat fluxes between chemical compositions
  - Chemical composition B (without CH_4) has marginal radiative influence

Wall heat fluxes - Aerocapture TP

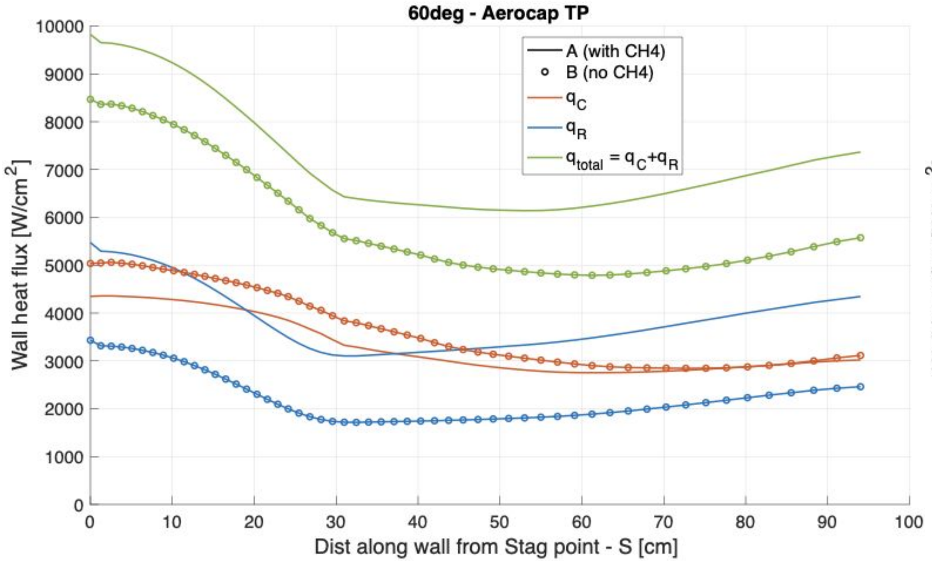

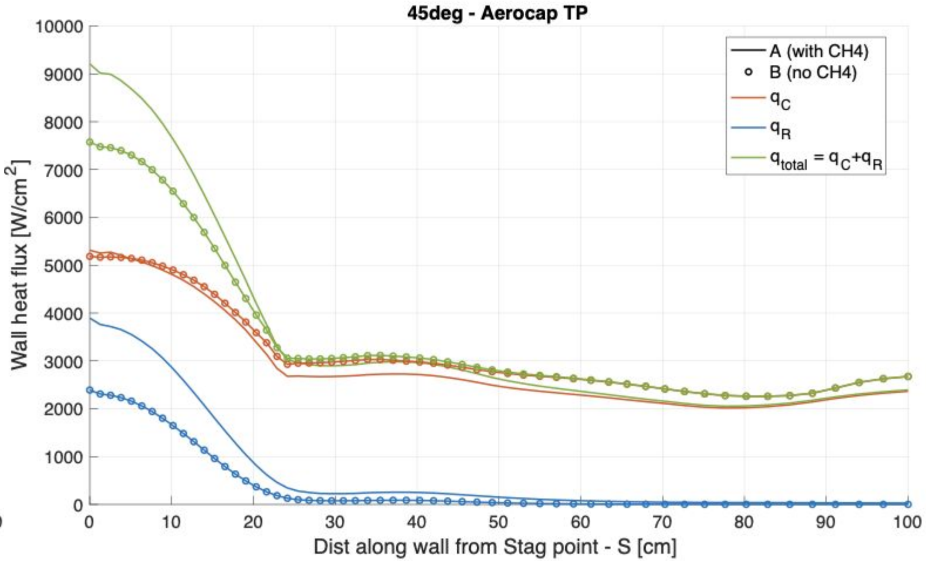

- Difference between chemical compositions in radiative heat fluxes is no longer critical
- Convective heat fluxes again similar with/without CH_4

Wall heat fluxes - Profile shapes

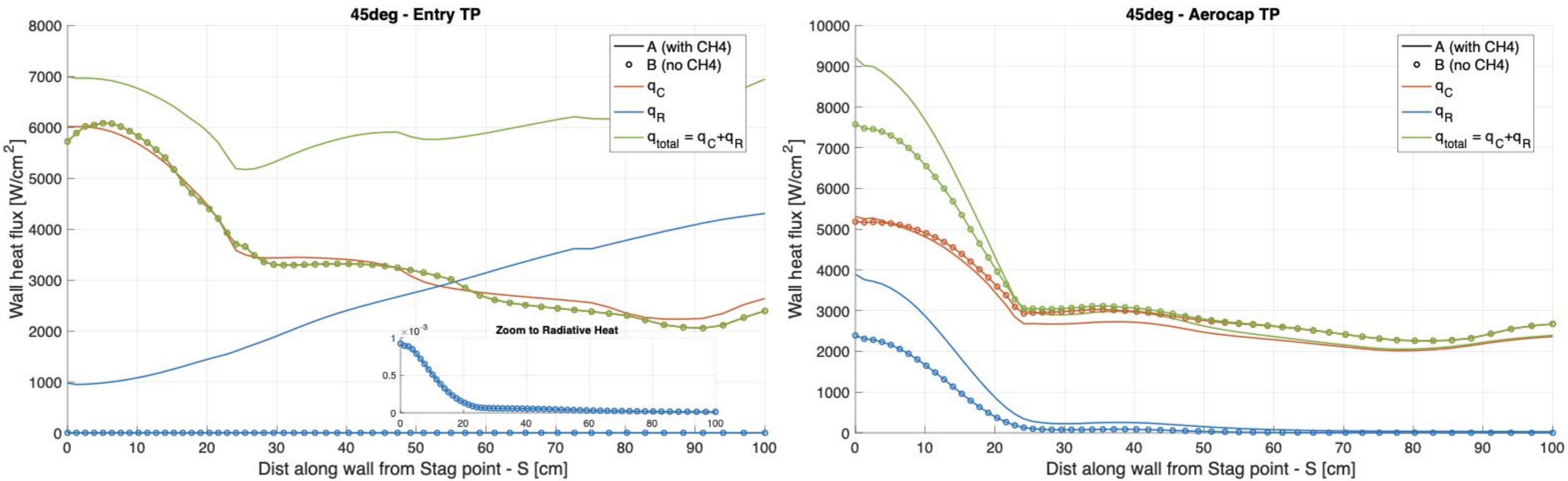

- Different profile shape for radiative heat fluxes (blue line)
  - Continuous growth for Entry TP
  - Higher values in the spherical part for Aerocapture TP

Wall heat fluxes - Profile shapes

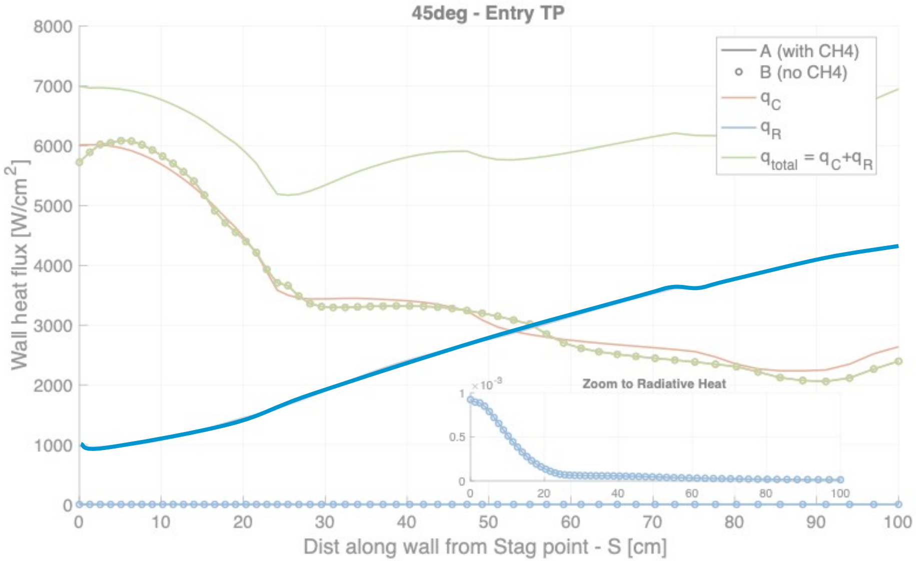

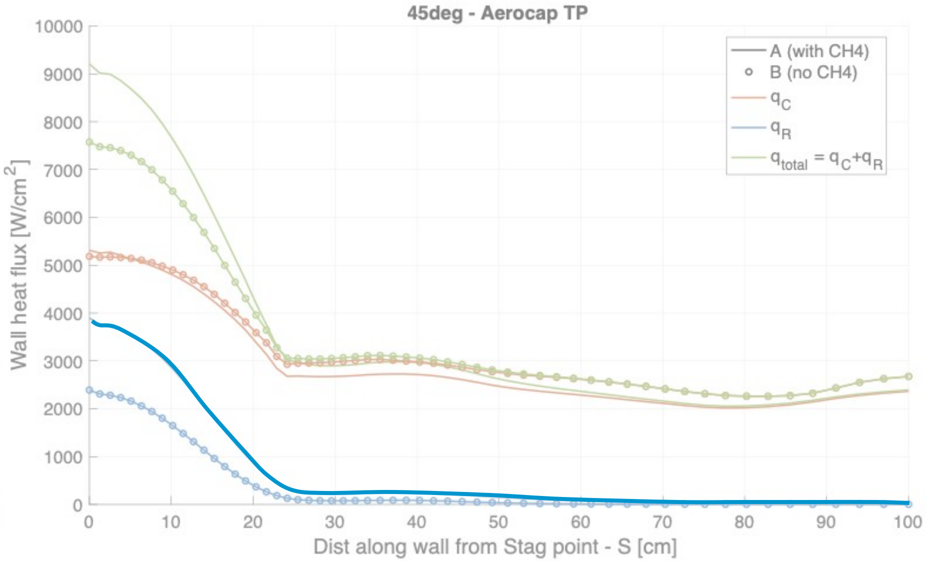

- Different profile shape for radiative heat fluxes (blue line)
  - Continuous growth for Entry TP
  - Higher values in the spherical part for Aerocapture TP

Temperature

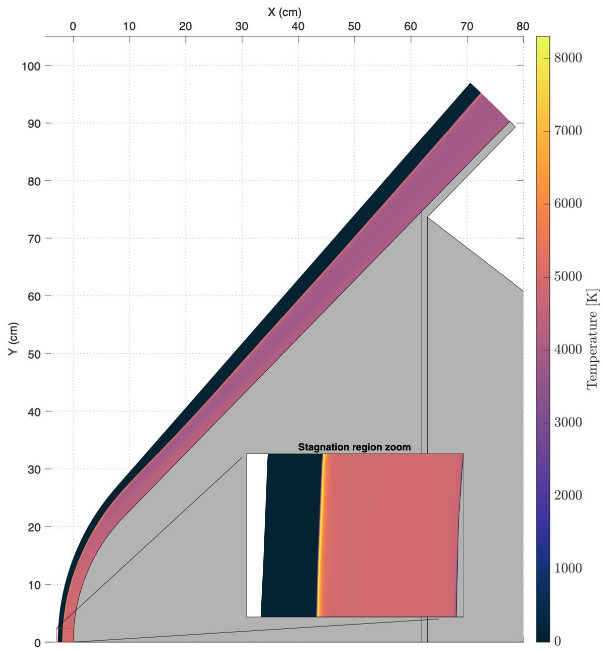

Entry TP

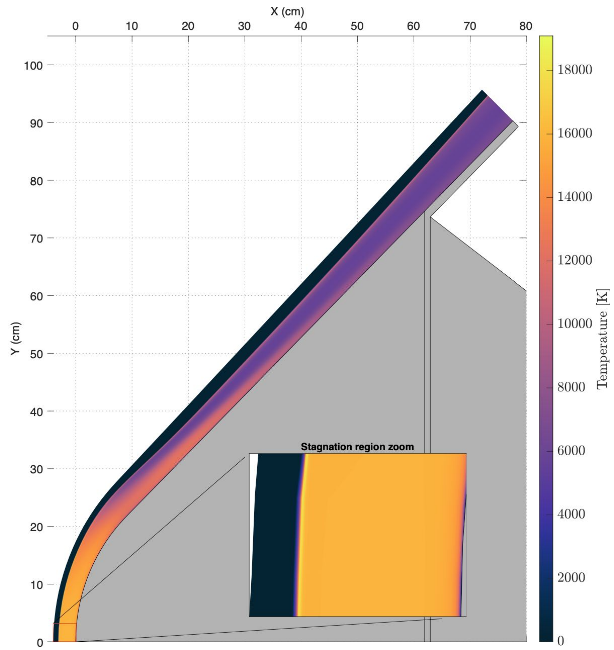

Aerocapture TP

- Temperature difference between stagnation region and near shoulder is more significant for Aerocapture TP (>10,000K) compared to Entry TP (<1,000K)

Radiative Power - Entry TP (with CH_4)

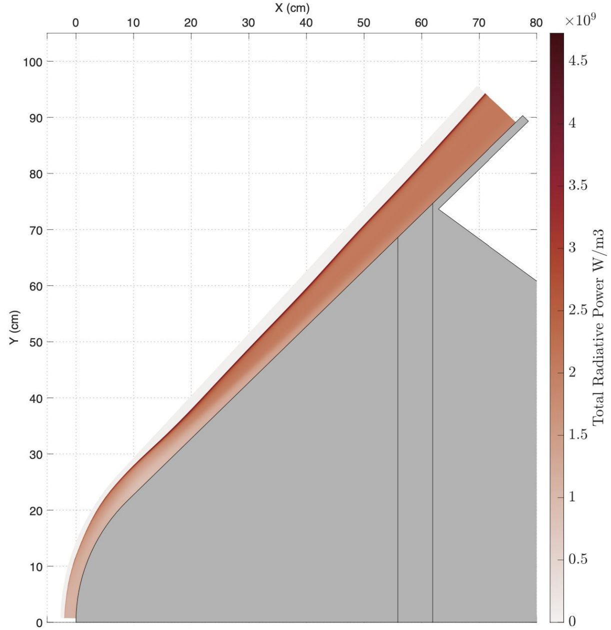

Total Radiative Power

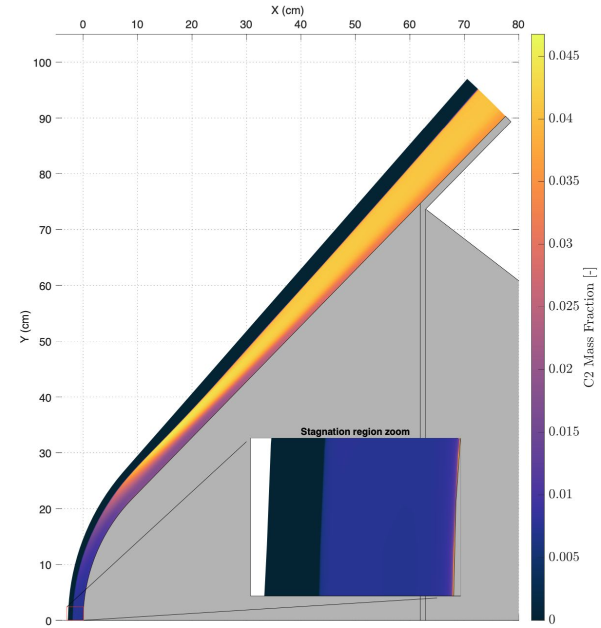

C2 Mass fraction

- C_2 concentration increases as we get farther from the stagnation region

Radiative Power - Entry TP (with CH_4)

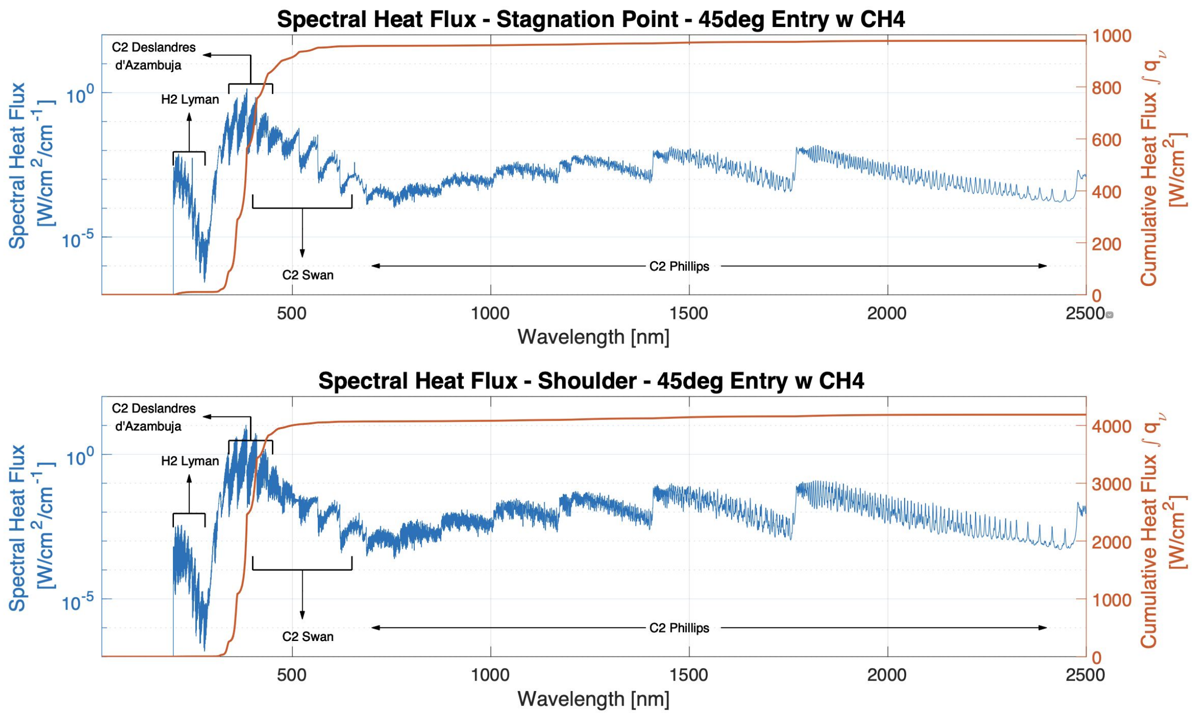

- C_2 radiative systems dominant in both locations

Radiative Power - Aerocapture TP (with CH_4)

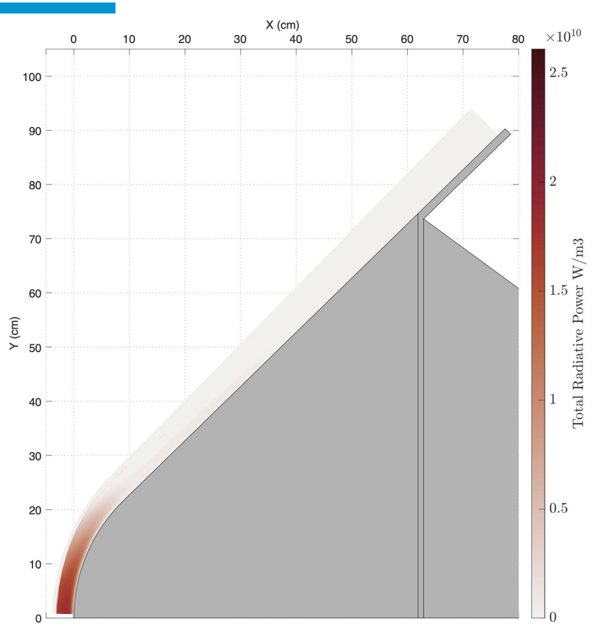

Total Radiative Power

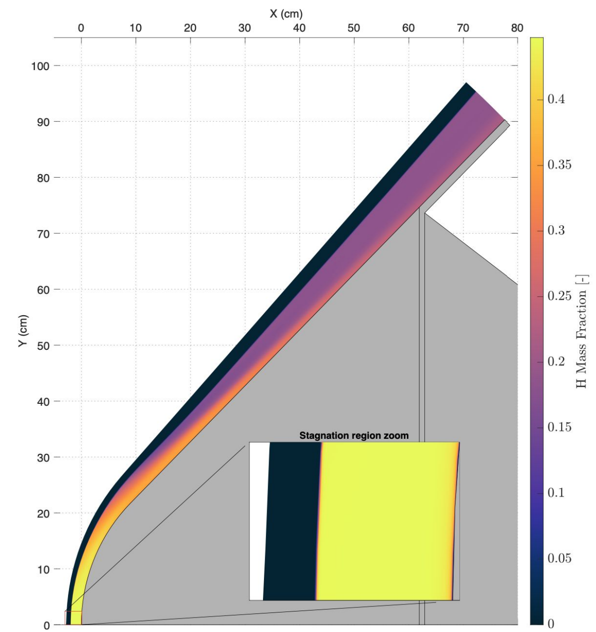

H mass fraction

- H concentration decreases as we get farther from the stagnation region
- Temperature has the main influence in the Radiative Power
  - Higher temperatures preclude the presence of molecular C_2 in the nose region
  - H (atomic) emits more radiation at higher temperatures

Radiative Power - Aerocapture TP (with CH_4)

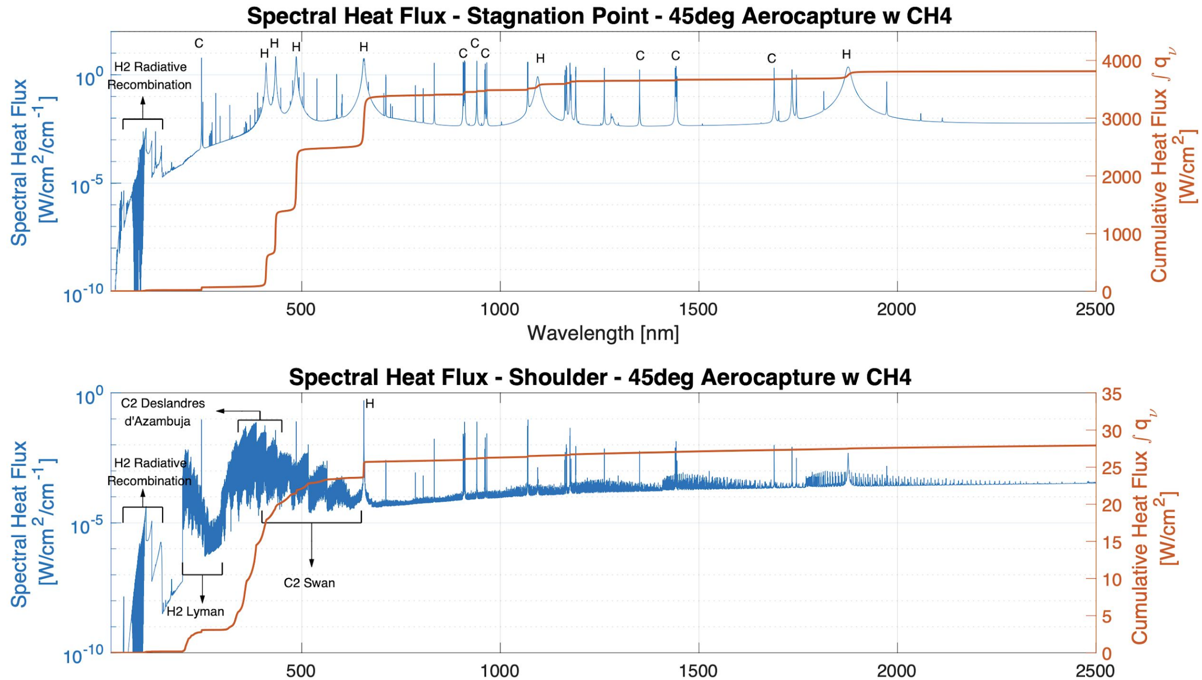

- Majority of spectral heat flux integration comes from H in the stagnation region.
- In the shoulder, lower temperatures:
  - H not emitting significantly
  - C_2 systems present, even though emitting at low magnitudes

Test case 2

Test case 2

- Only for Aerocapture TP
- Compute aerodynamic coefficients for both chemical configurations
- Evaluate sweep angle influence in the results

θ_c	Chemical Composition	η	Trajectory Point
60°	A and B	40° , 50° , 60° 70° , 80°	Aerocapture TP
45°	A and B	40° , 50° , 60° 70° , 80°	Aerocapture TP

Test Matrix for Test case 2

Approach

- Pressure correction
- Y-Force projection

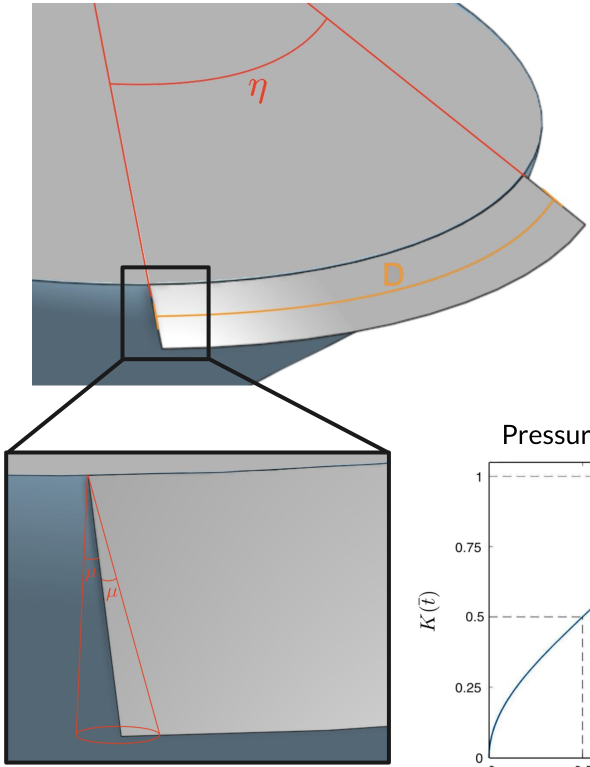

Mach cone

Pressure correction function

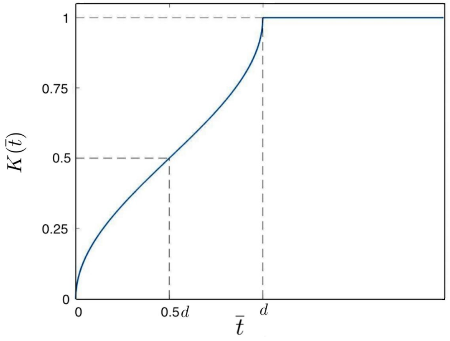

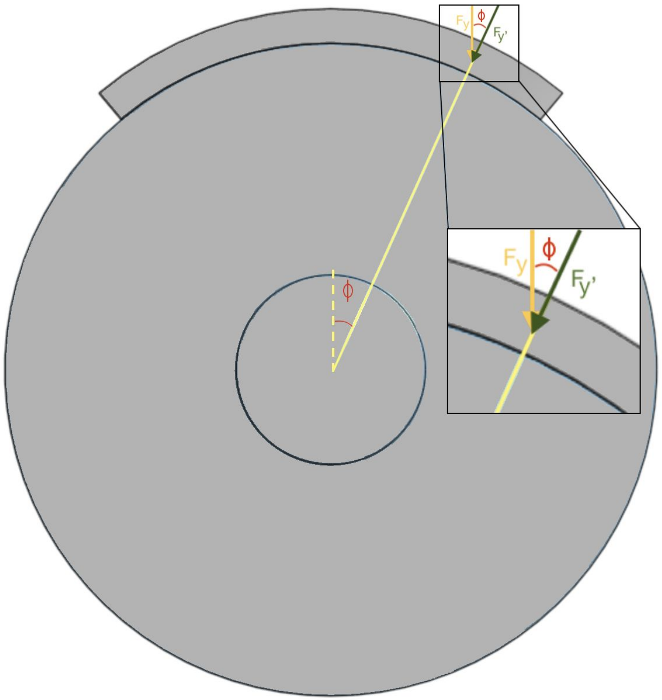

Aerodynamic coefficients

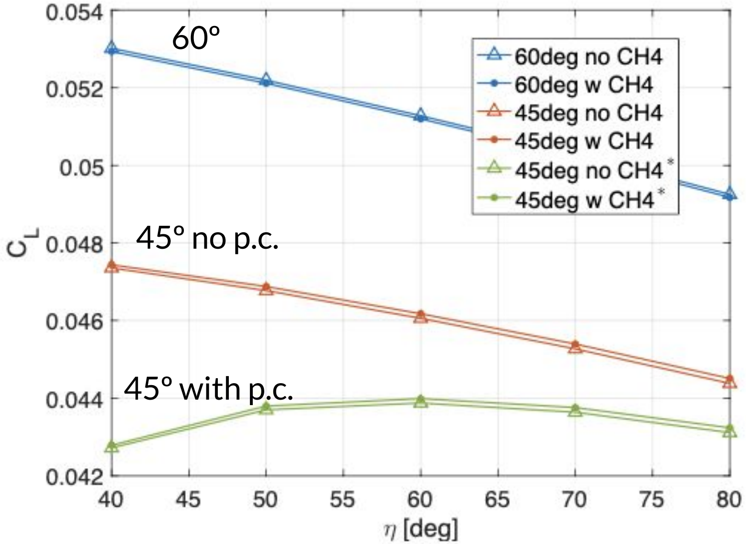

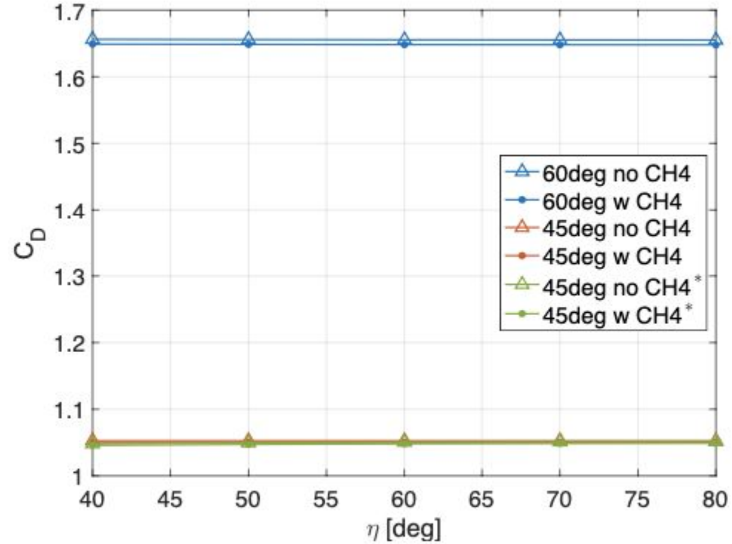

- Low influence of the chemical composition
- Pressure correction (*) larger impact on lower sweep angles
- Sweep angle marginal impact on the drag
- Low lift, but enough to produce a pitching moment
- Low influence of the viscous forces (0.0001% of the total)

8. Achievements and Future Work

Achievements

- CH_4 significantly enhances flow's radiation
  - At lower velocities the radiative heating starts being detrimental
  - At higher velocities provide also a smaller impact
- Instabilities for $\theta_c > 47°$ due to sonic line transition
  - $\theta_c = 45°$ capsule should be favored (following Galileo legacy)
    - Marginal advantages in the wall heating fluxes
    - Critical advantages in the stability

Future work

- Include the expansion region in the domain;
- Study with more detail the sonic line transition, together with angle of attack;
- Introduce the continuity of the second order derivative on the capsule's shape.

TÉCNICO LISBOA

THANK YOU FOR YOUR ATTENTION!

Major Achievements:

- CH_4 significantly enhances flow's radiation
  - Critical at lower velocities
- Instabilities for θ_c > 47° due to sonic line transition
  - 45° -> desired shape

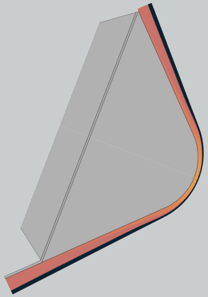

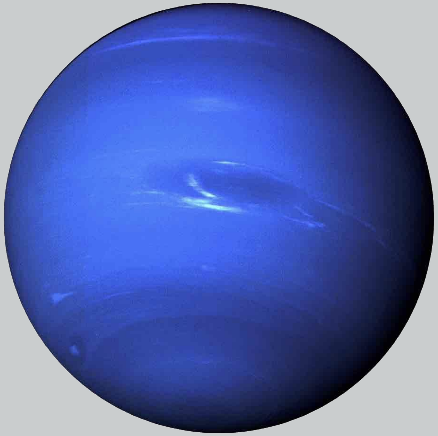

References

References

[1] M.M. Munk and S. Mood. ***Aerocapture Technology Development Overview.*** doi: 10.1109/AERO.2008.4526545

[2] M. S. Martin et al. ***In-flight experience of the Mars Science Laboratory Guidance, Navigation, and Control system for Entry, Descent, and Landing.*** doi:10.1007/s12567-015-0091-3

[3] L. Fernandes. ***Computational Fluid Radiative Dynamics of The Galileo Jupiter Entry at 47.5 km/s.*** Master's Thesis

[4] B.R. Hollis et al. ***Preliminary Convective-Radiative Heating Environments for a Neptune Aerocapture Mission.*** doi: 10.2514/6.2004-5177.

[5] S. Bayon and M. Bandecchi. ***CDF Study Report*** *- A Mission to the Ice Giants.* ESA Technical Report

[6] L.P. Leibowitz and T.-J. Kuo. ***Ionizational Nonequilibrium Heating During Outer Planetary Entries.*** doi: 10.2514/3.61465

[7] M. L. Silva et al. ***A Physically-Consistent Chemical Dataset for the Simulation of N2 – CH4 Shocked Flows Up to T = 100,000 K.*** Instituto Superior Técnico Technical Report

[8] A. Gonzalez. ***Measurement of Areas on a Sphere Using Fibonacci and Latitude-Longitude Lattices.*** doi: 10.1007/s11004-009-9257-x.